Status of the $R_K = \Gamma(K^{\pm}_{e2})/\Gamma(K^{\pm}_{\mu 2})$ measurement at the NA62 experiment

The NA62 collaboration[1]

Abstract

The current status of the R_K analysis based on the dedicated NA62 data set is summarized. The achieved precision of background subtraction, other systematic uncertainties, and prospects of the analysis are discussed.

Introduction

In the Standard Model (SM), charged leptons differ only by mass and coupling to the Higgs boson. However, SM extensions involving lepton flavour violation (LFV) are currently not ruled out by experiment. A possible method to search for LFV is by precise measurements of the ratios of coupling constants for different types of leptons, seeking for deviations from unity in processes well known in the SM.

The SM predictions for the ratios of purely leptonic decay rates of K and π mesons reach excellent sub-permille accuracy, profiting from cancellations of the hadronic uncertainties [1]. Measurements of these quantities, in particular $R_K = \Gamma(K^{\pm}_{e2})/\Gamma(K^{\pm}_{\mu 2})$, have been traditionally (since the first observation of the $\pi^+ \to e^+\nu$ decay at CERN in 1958) considered as tests of lepton universality.

By convention, the inner bremsstrahlung (IB) part of the radiative $K_{\ell 2\gamma}$ process is included into R_K, while the structure dependent (SD) $K_{\ell 2\gamma}$ process (which can not be accurately computed) is not. The SM prediction [1] has an excellent precision:

$$R_K^{\mathrm{SM}} = \left(\frac{m_e}{m_\mu}\right)^2 \left(\frac{m_K^2 - m_e^2}{m_K^2 - m_\mu^2}\right)^2 (1 + \delta R_{\mathrm{QED}}) = (2.477 \pm 0.001) \times 10^{-5}. \qquad (1)$$

Here $\delta R_{\mathrm{QED}} = (-3.78 \pm 0.04)\%$ is a correction due to the IB radiative process. The factor $(m_e/m_\mu)^2$ accounts for the helicity suppression of the K_{e2} decay due to the $V - A$ structure of the charged weak current.

The above helicity suppression enhances the sensitivity to non-SM effects. In particular, enhancement of R_K by a few percent (relative) is quite possible in minimal supersymmetric extensions of the SM, and is expected to be dominated by LFV (rather than LFC) contributions with emission of the tau neutrino [2, 3], with no contradiction to any

[1]Corresponding author: Evgueni Goudzovski, email: eg@hep.ph.bham.ac.uk.

presently known experimental constraints (including upper bounds on the rare $\tau \to eX$ decays with $X = \gamma, \eta, \mu\mu$). On the other hand, analogous SUSY effects in the $\pi_{e2}/\pi_{\mu 2}$ rates ratio is suppressed by a factor of $(m_\pi/m_K)^4 \approx 6 \times 10^{-3}$.

The helicity suppression of the K_{e2} decay naturally poses experimental difficulties in measuring it. The current world average $R_K^{\rm PDG} = (2.45 \pm 0.11) \times 10^{-5}$ [4] dates back to three experiments performed in the 1970s, and has insufficient precision (4.5%) for stringent SM tests. A series of recent preliminary results from NA48/2 and KLOE represents a significant improvement. Combining these results with the PDG value yields a 1.3% precision: $R_K^{\rm exp} = (2.457 \pm 0.032) \times 10^{-5}$ [5].

The aim of the NA62 experimental programme based on the 2007 data set is a measurement of R_K reaching a new accuracy level better than 0.4% [6]. To achieve this goal, data taking strategy allowing control over the systematic effects, in particular precise background subtraction, was worked out, and a record data sample of $\sim 0.16 \times 10^6$ K_{e2} candidates with just $\sim 10\%$ background was collected.

1 Beams, detector and data taking

The NA48/2 beam line and setup were used during the 2007 K_{e2} run. Running conditions were significantly optimized for the K_{e2} measurement using the experience of the earlier NA48/2 K_{e2} studies based on 2003 and 2004 test data sets [7].

Kaon beams

The beam line is capable of delivering simultaneous narrow momentum band K^+ and K^- beams; a central momentum 75 GeV/c was used in 2007. The K^+/π^+ ratio at the entrance to the decay volume was measured to be $(8.6 \pm 0.2)\%$. Momentum of the incoming kaon is not measured directly for each event; the beam average monitored with $K^\pm \to 3\pi^\pm$ decays is used to reconstruct K_{l2} kinematics by missing mass $M_{\rm miss}$. A narrow momentum spectrum ($\Delta p_K^{\rm RMS}/p_K \approx 2\%$) is used to minimize the corresponding contribution to the $M_{\rm miss}$ resolution.

The K_{l2} decay signature consists of a single reconstructed track, thus the background in K_{l2} samples induced by the beam halo becomes an important issue. The performance of the muon sweeping system is such that the K_{e2}^- sample is more heavily affected than the K_{e2}^+ one (contaminations are $\sim 20\%$ and $\sim 1\%$, respectively). Therefore most of the data were taken with the K^+ beam only (with the K^- beam dumped upstream the decay volume). Conversely, about 10% of the data were recorded with the K^- beam only. Samples of reconstructed K_{l2} candidates of the charge not present in the beam provide measurements of the halo background. Thus the separate K^+ and K^- samples allow for cross-subraction of the halo background with precisions much better than statistical uncertainty of the measurement.

Detector and trigger

The following subdetectors located downstream a vacuum decay volume are principal for the R_K measurement.

- A magnetic spectrometer composed of four drift chambers (DCHs) and a spectrometric magnet (MNP33) used to detect charged products of kaon decays. Each

chamber is composed of eight planes of sense wires arranged in four pairs of staggered planes. The resolution on track momentum is $\delta p/p = 0.47\% \oplus 0.020\% p$ (where p is expressed in GeV/c).

- A plastic scintillator hodoscope (HOD) used to produce fast trigger signals. The HOD consists of a plane of vertical and a plane of horizontal strip-shaped counters, each plane comprising 64 counters arranged in four quadrants.

- A liquid krypton (LKr) electromagnetic calorimeter used for γ detection and particle identification. It is an almost homogeneous ionization chamber with an active volume of 7 m^3 of krypton, $27X_0$ deep, segmented transversally into 13,248 projective cells (2×2 cm^2 each), and with no longitudinal segmentation.

A beam pipe traversing the centres of the detectors allows undecayed beam particles and muons from decays of beam pions to continue their path in vacuum.

A minimum bias trigger configuration was employed, resulting in relatively low trigger purities, but, importantly, high efficiencies. The K_{e2} trigger condition consisted of a time coincidence of hits in the two planes of the HOD (the so called Q_1 signal) with an energy deposition of at least 10 GeV in the LKr. The $K_{\mu2}$ trigger condition consisted of the Q_1 signal alone downscaled by a factor ranging from 50 to 150. Very loose requirements on the activity in the DCHs were additionally included into the trigger logic to enhance its purity against high multiplicity events.

Data taking

The main data sample was taken during four months of running in 2007 (23/06 till 22/10). About 0.4×10^6 SPS spills were recorded; the data recording system handled about 300 TB of raw data, of which 90 TB were recorded on tape after Level III (software) trigger reduction. Reprocessing of these data involving, in particular, calibration of the subdetectors was mostly finished by September 2008.

Two additional weeks of data taking were allocated in 2008 (11/09 till 24/09). The beam time was efficiently used to collect several special data samples, which are expected to contribute significantly to the reduction of the systematic uncertainties.

2 Data analysis

As the first stage of the analysis, about 40% of the total data sample (corresponding to about 60K K_{e2} candidates) collected with the K^+ beam only are currently being analyzed. A detailed Monte Carlo (MC) simulation including full detector geometry and material description, DCH local inefficiencies, detailed simulation of the kaon beam line, and time variations of the above throughout the running period has been tuned to describe these data.

Measurement method

The analysis strategy is based on counting the numbers of reconstructed K_{e2} and $K_{\mu2}$ candidates collected simultaneously, consequently 1) the result does not rely on kaon flux measurement; 2) several systematic effects, such as parts of the trigger and detection efficiencies, cancel in the ratio. MC simulations are used to a limited extent only: 1)

to evaluate a correction for the difference of K_{e2} and $K_{\mu 2}$ geometric acceptances; 2) to simulate of a particular effect of energetic bremsstrahlung by a muon, which is not directly accessible experimentally, as discussed below. Efficiencies of trigger conditions and particle identification criteria are measured directly.

The analysis is performed independently in bins of the reconstructed momentum of the charged track, due to strong dependence of the backgrounds and acceptance on this variable. The ratio R_K in each momentum bin is computed as

$$R_K = \frac{1}{D} \cdot \frac{N(K_{e2}) - N_{\rm B}(K_{e2})}{N(K_{\mu 2}) - N_{\rm B}(K_{\mu 2})} \cdot \frac{f_\mu \times A(K_{\mu 2}) \times \epsilon(K_{\mu 2})}{f_e \times A(K_{e2}) \times \epsilon(K_{e2})} \cdot \frac{1}{f_{\rm LKr}}, \tag{2}$$

where $N(K_{\ell 2})$ are the numbers of selected $K_{\ell 2}$ candidates ($\ell = e, \mu$), $N_{\rm B}(K_{\ell 2})$ are numbers of background events, f_ℓ are efficiencies of e/μ identification criteria, $A(K_{\ell 2})$ are the geometrical acceptances computed with MC, $\epsilon_{\rm trig}$ are trigger efficiencies, $f_{\rm LKr}$ is the global inefficiency of the LKr readout, and D is the downscaling factor of the $K_{\mu 2}$ trigger.

Event selection

Due to the topological similarity of K_{e2} and $K_{\mu 2}$ decays, a large part of the selection conditions is common for both decays, which leads to cancellations of the related systematic uncertainties in R_K. The principal selection requirements are presented below.

- Exactly one charged particle track reconstructed by the spectrometer: $N_{\rm track} = 1$.
- Extrapolated impact points of the track in the DCHs, LKr calorimeter and HOD are within their geometrical acceptance.
- No LKr energy deposition clusters with energy $E > 2$ GeV and not associated to the track, which suppresses background from other kaon decays.
- The decay vertex is reconstructed as the point of closest approach between the charged track and the nominal kaon beam axis. The closest distance of approach is required not to exceed 2 cm, and the vertex longitudinal coordinate to be at least 18 m downstream the final collimator (the latter is required to suppress the beam halo background).
- Reconstructed track momentum: 15 GeV/c $< p <$ 65 GeV/c. The lower limit is due to the requirement of at least 10 GeV energy deposit in the LKr calorimeter in the K_{e2} trigger condition, while the upper limit is close to the kinematical limit.

The following two principal selection criteria are different for the K_{e2} and $K_{\mu 2}$ decays.

- Kinematical $K_{\ell 2}$ identification is based on reconstruction of the squared missing mass assuming the track to be an electron or a muon:

$$M^2_{\rm miss}(\ell) = (P_K - P_\ell)^2, \tag{3}$$

  where P_K, P_ℓ ($\ell = e, \mu$) are the kaon four-momentum (average beam momentum assumed) and lepton four-momentum (electron or muon mass assumed). A cut $|M^2_{\rm miss}(e)| < 0.01$ (GeV/c^2)^2 is applied to select K_{e2} candidates, and $|M^2_{\rm miss}(\mu)| <$ 0.01 (GeV/c^2)^2 for $K_{\mu 2}$ ones.

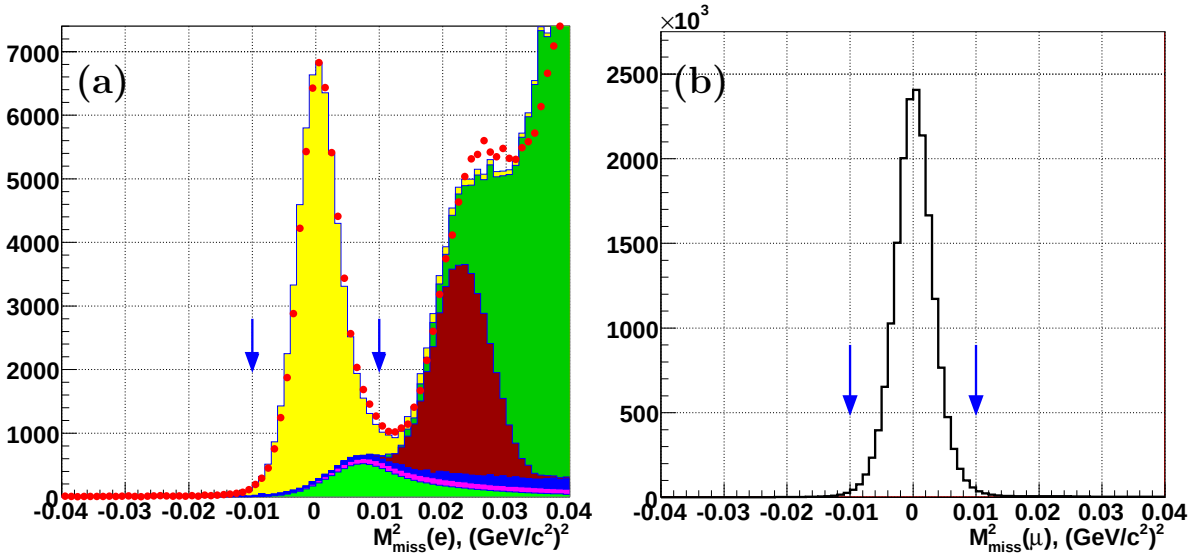

Figure 1: Reconstructed squared missing mass distributions (signal regions are marked with arrows). (a) $M^2_{\rm miss}(e)$ for K_{e2} candidates. Data (dots) and expectations for background and signal (filled areas). Layers from bottom to top: $K_{\mu 2}$, $K_{e2\gamma}$ (SD), beam halo, $K_{2\pi}$, K_{e3}, K_{e2}. (b) $M^2_{\rm miss}(\mu)$ for $K_{\mu 2}$ candidates.

- Particle identification is based on the ratio E/p of track energy deposit in the LKr to its momentum measured by the spectrometer. Particles with $0.95 < E/p < 1.05$ ($E/p < 0.2$) are identified as electrons (muons).

The above selection yields the following numbers of $K_{\ell 2}$ candidates: $N(K_{e2}) = 59,293$ and $N(K_{\mu 2}) = 17,662,856$. The corresponding squared missing mass distributions are presented in Fig. 1. For comparison, the previous world's largest sample K_{e2} sample collected by the KLOE experiment is 8,090 candidates (after background subtraction).

Muonic background in the K_{e2} sample

The background in the K_{e2} sample originating from the $K_{\mu 2}$ decays represents one of the central issues of the analysis. As shown in Fig. 2, sufficient kinematical suppression of K_{e2} and $K_{\mu 2}$ decays in the region of high lepton momentum ($p > 40$ GeV/c) is not achievable. On the other hand, a muon can fake an electron in terms of particle identification, depositing over 95% of its energy in the LKr calorimeter by 'catastrophic' bremsstrahlung. The probability of such process in the NA62 experimental conditions $P(\mu \to e) \sim 3 \times 10^{-6}$, though relatively small, is non-negligible in comparison to the expected value of $R_K^{\rm SM} = 2.477 \times 10^{-5}$, making the $K_{\mu 2}$ decay a major background source for K_{e2}.

A direct measurement of $P(\mu \to e)$ with a few percent precision is a necessary requirement for validation of the theoretical computation of the bremsstrahlung cross-section [8] in the highly energetic γ range used to evaluate the $K_{\mu 2}$ background. Typical NA62 muon samples have $\sim 10^{-4}$ electron contaminations due to $\mu \to e$ decays in flight, while a contamination much lower than the value of $P(\mu \to e)$ is required for its measurement. To collect sufficiently pure muon samples, a $\sim 10X_0$ thick lead wall covering about 20% of the HOD geometric acceptance was installed between the two HOD planes during certain periods of the data taking. In the samples of tracks passing through the lead wall and

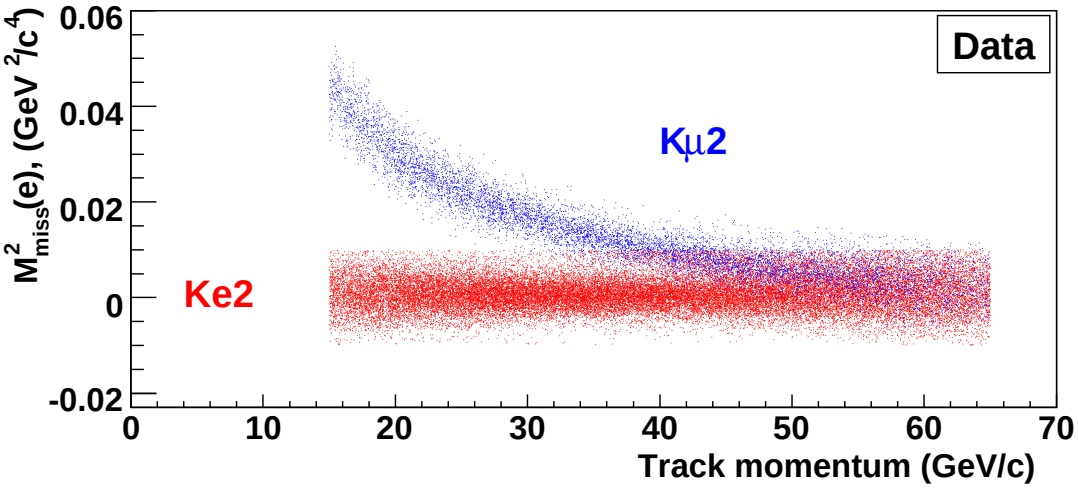

Figure 2: Missing mass squared in electron hypothesis $M^2_{\rm miss}(e)$ vs track momentum for reconstructed K_{e2} and $K_{\mu 2}$ decays. Good kinematic separation of K_{e2} and $K_{\mu 2}$ decays is possible at low track momentum only.

depositing over 95% of their energy in the LKr calorimeter, the electron component is suppressed to the desirable level by the high electron energy loss in the wall, while the muon component is affected weakly.

The following pure muon samples with high E/p were collected: 1) from the $K_{\mu 2}$ decays during the main data taking with K beams; 2) from special muon runs with the hadron beam absorbed upstream the decay volume. The present analysis uses only a muon sample collected during a 20h special muon run on 2007 containing over 1,500 muons in the poor $K_{e2}/K_{\mu 2}$ kinematical separation range (35 GeV/c $< p <$ 65 GeV/c) traversing the lead wall and faking electrons by $0.95 < E/p < 1.05$. The 2008 special muon sample, not used in the present analysis, contains about twice as many muons.

The momentum dependence of $P(\mu \to e)$ measured with the lead wall technique is presented in Fig. 3 in comparison to the results of a dedicated Geant4-based MC simulation (with and without the lead wall) involving, along with the standard muon energy loss processes, the theoretical bremsstrahlung cross-section [8], and the subsequent electromagnetic shower development. Results of the simulation of a setup with the lead wall are in excellent agreement with the measurement in a wide momentum range within data statistical errors, which validates the model describing the cross-section. The simulation also demonstrates that the presence of the lead wall appreciably modifies $P(\mu \to e)$ via the following principal mechanisms: 1) muon energy loss in the lead by ionization decreasing $P(\mu \to e)$ and dominating at low momentum; 2) 'catastrophic' bremsstrahlung in the lead increasing $P(\mu \to e)$ and dominating at high momentum.

To estimate the $K_{\mu 2}$ background contamination, the kinematic suppression factor is computed with the standard Geant3-based simulation of the setup, while the validated Geant4-based simulation of muon interaction in the LKr (without the lead wall) is employed to account for the particle ID suppression. The preliminary result for the background to signal ratio is $B/S = (8.07 \pm 0.21)\%$; background is located at high track momentum due to the poor $K_{e2}/K_{\mu 2}$ kinematic separation there. The uncertainty of B/S is due to the limited size of the data sample used to validate the simulation with the lead wall.

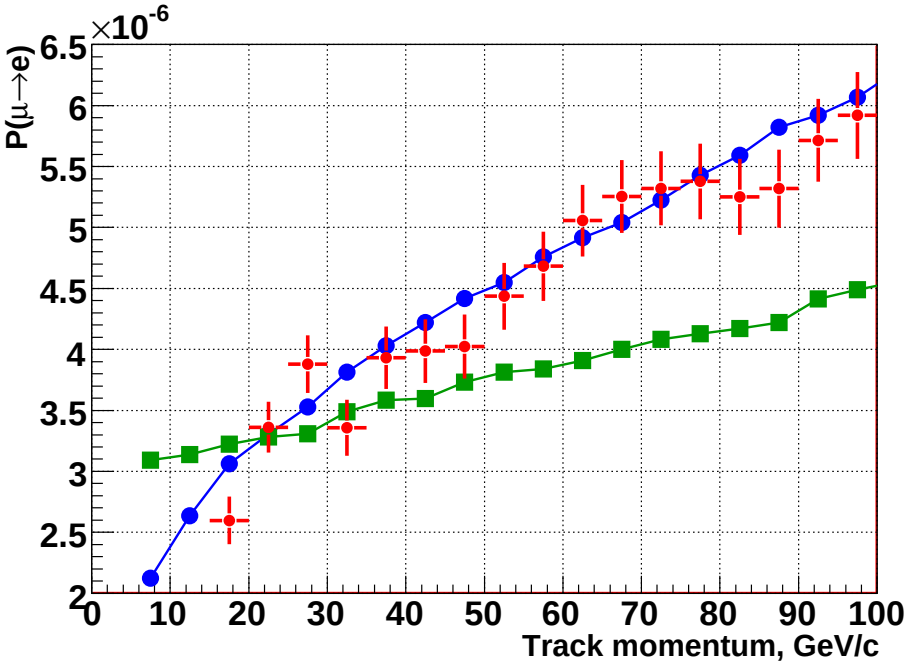

Figure 3: Measured and simulated probability of muon identification as an electron $P(\mu \to e)$ vs track momentum. Points with error bars: data with Pb wall, circles: MC with Pb wall, squared: MC without Pb wall.

Analysis of the other muon samples, especially the large special 2008 sample, is expected to improve the precision of the estimation. Another tool for $P(\mu \to e)$ study is provided by the pure sample of muons from the $K_{\mu 2}$ decays not traversing the lead wall selected kinematically in the track momentum region of good kinematic $K_{e2}/K_{\mu 2}$ separation ($p < 25$ GeV/c). This sample can be used for an independent cross-check of the lead wall technique, and testing geometrical uniformity of the LKr calorimeter response.

$K_{e2\gamma}$ background

The rate of the structure-dependent (SD) $K_{e2\gamma}$ decay, which is considered a background by the definition of R_K, is of similar magnitude to that of K_{e2}: theoretical prediction for its BR ranges from 1.12×10^{-5} to 1.34×10^{-5}, depending on the model for kinematical dependence of the form factor [9]. The experimental precision is similar: BR $= (1.52 \pm 0.23) \times 10^{-5}$ [4], where uncertainty due to model dependence is not taken into account.

Only the part of $K_{e2\gamma}$ (SD) phase space with high electron energy in kaon rest frame ($E_e^* \gtrsim 230$ MeV) is compatible to K_{e2} kinematic identification, and contributes to the background via the γ escaping detector acceptance. The background contamination is estimated by MC simulation to be $B/S = (1.29 \pm 0.32)\%$; its uncertainty is due to the limited experimental and theoretical knowledge of the process mentioned above. Fortunately the relevant $K_{e2\gamma}$ kinematic region is accessible for a model-independent BR measurement, being above the upper kinematic limit ($E_e^* = 227$ MeV) of the K_{e3} background. Such measurement based on the NA62 2007 data sample has started, and is expected to improve the corresponding systematic uncertainty on R_K.

Beam halo background

The background contamination in the K_{e2} sample induced by beam halo muons under-

Source	Background/signal ratio
$K_{\mu 2}$	$(8.07 \pm 0.21)\%$
$K_{e2\gamma}$ (SD)	$(1.29 \pm 0.32)\%$
Beam halo	$(1.23 \pm 0.07)\%$
$K_{2\pi}$	$\sim 0.1\%$
K_{e3}	$\sim 0.03\%$
$K_{\mu 2}$ + accidentals	$\sim 0.1\%$
Sum of 3 main contributions	$(10.59 \pm 0.39)\%$

Table 1: Summary of backgrounds to the K_{e2} decay.

going $\mu \to e$ decays in flight, with the produced electron being kinematically and geometrically compatible to a genuine K_{e2} decay, is directly measured with the 2007 K^- only sample to be $B/S = (1.23 \pm 0.07)\%$. The rate and kinematical distribution of this background are fairly well reproduced by simulation of the muon halo.

The uncertainty of B/S is reasonably small, and is due to the limited size of the K^- sample. An additional K^- only sample collected in 2008, which is about half the size of the 2007 sample, will allow a further improvement of the uncertainty. The smallness of the current uncertainty potentially allows expanding the analysis fiducial decay volume upstream (into the region of higher halo background contamination), which would increase the data sample by an amount of the order of 10%.

Beam halo background contamination in the $K_{\mu 2}$ sample is measured to be 0.14% with the same technique as for K_{e2} decays. The uncertainty of the measurement is negligible, not limited by the size of the control sample as in the K_{e2} case.

Other identified backgrounds

Two minor background sources in the K_{e2} sample due to kaon decays identified with MC simulations are $K^+ \to \pi^0 e^+ \nu$ (so called K_{e3}) and $K^\pm \to \pi^\pm \pi^0$ (so called $K_{2\pi}$) decays. The preliminary conclusion from simulations is that they contribute at a level below 0.1%.

Another mechanism by which a muon is identified as an electron ($E/p > 0.95$) is due to an accidental LKr energy deposition cluster found close to muon impact position. This background is directly measured using sidebands of track-cluster timing and distance distributions to be at the level of 0.1%.

The $K_{2\pi}$ was identified to be a sources of background in the $K_{\mu 2}$ sample. Its contamination is below 0.1%, as was established by MC simulation.

Summary of the backgrounds

The backgrounds in the K_{e2} sample are summarized in Table 1, and indicated in Fig. 1a. The three main backgrounds ($K_{\mu 2}$, $K_{e2\gamma}$ and beam halo) currently introduce a 0.4% uncertainty to R_K, however precision of estimation of each of them is going to be improved, as discussed above in detail. Precise computations of the minor backgrounds and their uncertainties are in progress. Distribution of the main backgrounds to K_{e2} in bins of track momentum is presented in Fig. 4: they mostly contribute at high track momentum.

Other systematic effects

Geometric acceptance correction $A(K_{\mu 2})/A(K_{e2})$ is momentum dependent, and ranges between 1.2 and 1.4 in the analysis momentum interval. The correction is strongly in-

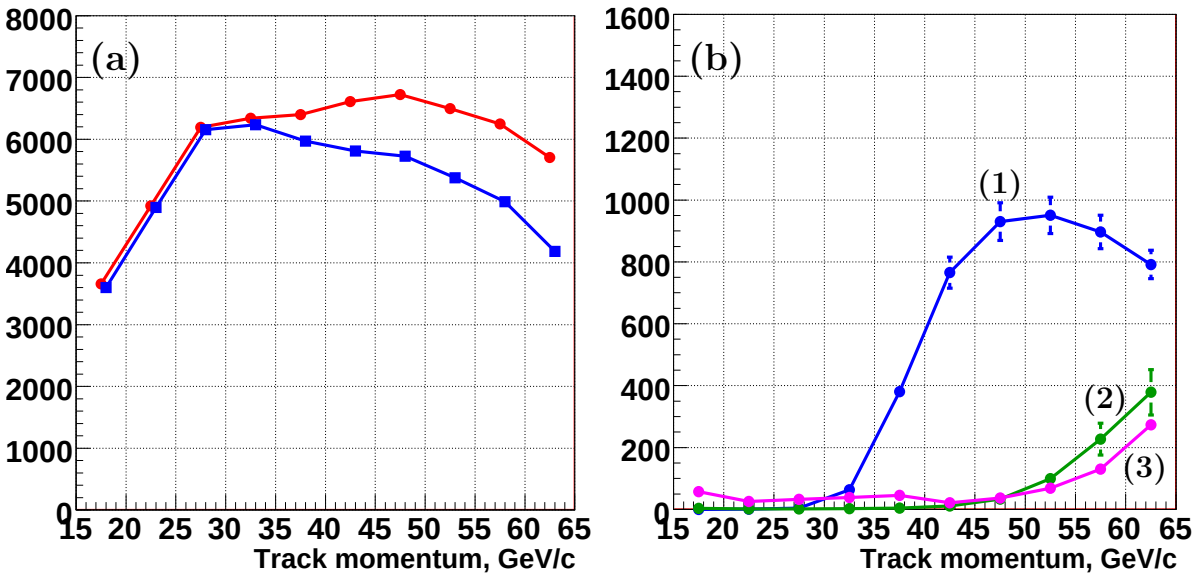

Figure 4: (a) Numbers of K_{e2} candidates in track momentum bins: raw (circles) and after background subtraction (squares). (b) Distribution of the main backgrounds over track momentum bins: (1) $K_{\mu 2}$; (2) $K_{e2\gamma}$ (SD), (3) beam halo.

fluenced by the radiative $K_{e2\gamma}$ (IB) decays. Previous experience suggests that the MC correction factor can be evaluated with a precision better than 0.1%.

Electron identification efficiency (including its dependence on track momentum and impact point position) is directly measured with a clean sample of electrons obtained by kinematic selection of $K^{\pm} \to \pi^0 e^{\pm} \nu$ decays collected simultaneously with the main $K^{\pm}$ data sample (in a limited kinematic region $p < 50$ GeV/c), and a sample of electrons obtained by kinematic selection of $K_L \to \pi^{\pm} e^{\mp} \nu$ decays from a special 15h run with a broad momentum spectrum K_L beam (in the whole analysis p range). The measured efficiency f_e is close to 99%, and has weak momentum dependence, as presented in Fig. 5. The precision of f_e measurement is better than 0.1%.

Muon identification efficiency f_μ is measured with a pure muon sample from a special muon run to range from 0.996 to 0.999 in the analysis track momentum region, as presented in Fig. 5. The precision of the measurement is much better than 0.1%. The f_μ measurement is considerably more simple than that of $P(\mu \to e)$, since the electron contamination in a muon sample is outside the muon identification range of $E/p < 0.2$.

Trigger efficiency correction $\epsilon(K_{\mu 2})/\epsilon(K_{e2})$ is required mainly due to the fact that K_{e2} and $K_{\mu 2}$ decay modes are collected with different trigger conditions: the $E > 10$ GeV LKr energy deposition signal enters the K_{e2} trigger condition only. Its efficiency in the signal momentum interval $p > 15$ GeV/c is measured directly using a control data set to be below 0.1%.

Finally, the global LKr calorimeter readout inefficiency $f_{\rm LKr}$ is about 0.2%, according to a series of preliminary measurements. Effects of trigger afterpulses biasing the $K_{\mu 2}$ trigger downscaling factor D are expected not to exceed 0.1%.

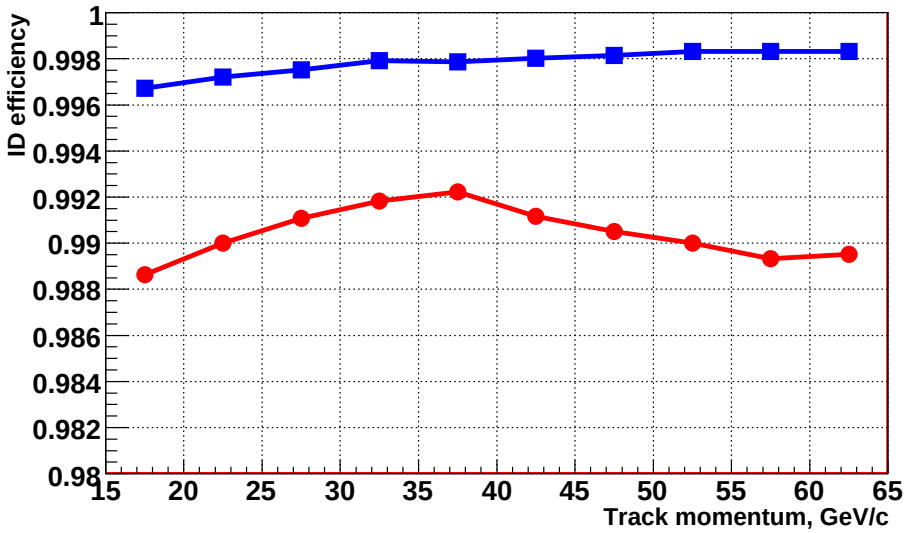

Figure 5: Momentum dependencies of the measured electron (circles) and muon (squares) mis-identification probabilities f_e and f_μ in the analysis momentum range.

Source	$(\delta R_K/R_K) \times 10^2$
Statistical	0.43
$K_{\mu 2}$	0.25
$K_{e2\gamma}$ (SD)	0.32
Beam halo	0.10
Total	0.60

Table 2: Uncertainty of R_K: statistical and main systematic contributions.

3 Summary and prospects

The independent measurements of R_K in track momentum bins with are presented in Fig. 6, with an overall offset artificially applied to set the result to the SM expectation. The stability of R_K over momentum bins points to good control over the main systematic effects, in view of the size and momentum dependence of the backgrounds (Fig. 4b) and the acceptance correction. The statistical error and main systematic uncertainties (coming from subtraction of main backgrounds) are listed in Table 2. A number of smaller uncertainties discussed above, but not yet fully evaluated, are not presented yet.

The analysis demonstrates that the main systematic effects are under good control. Further studies of second-order effects and minor background sources are currently underway in order to finalize the measurement of R_K with the currently considered partial 40% data sample. The total uncertainty of the partial result is expected to be 0.6–0.7%, breaking the 1% level for the first time.

The whole NA62 data sample of ∼160K K_{e2} decay candidates, which is an order of magnitude larger than the world sample, allows pushing the statistical uncertainty to a level below 0.3%. Significant improvements of the $K_{\mu 2}$ background and beam halo systematic uncertainties are possible thanks to the special data sets collected during the K_{e2} systematics run in 2008. The uncertainty due to the $K_{e2\gamma}$ (SD) background is expected to be decreased by a direct measurement of this process. The ultimate precision of the measurement is expected to reach the 0.4% level, meeting the goal declared in the proposal [6].

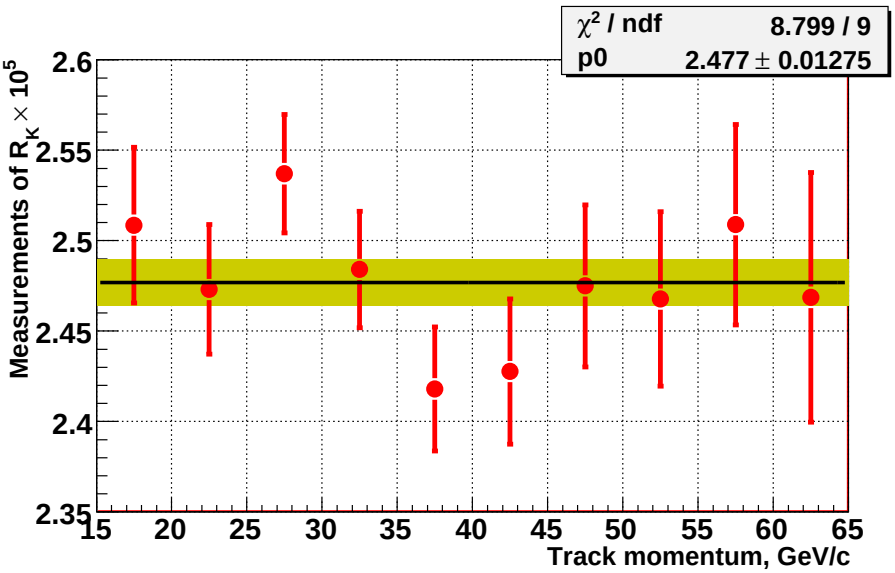

Figure 6: Independent measurements of R_K in momentum bins, with an overall offset artificially applied to hide the result setting it to the SM expectation. Uncertainties due to $K_{e2\gamma}$ background correlated between momentum bins are excluded.

References

[1] V. Cirigliano and I. Rosell, Phys. Rev. Lett. **99** (2007) 231801.

[2] A. Masiero, P. Paradisi and R. Petronzio, Phys. Rev. **D74** (2006) 011701.

[3] A. Masiero, P. Paradisi and R. Petronzio, arXiv:0807.4721.

[4] C. Amsler *et al.* (PDG), Phys. Lett. **B667** (2008) 1.

[5] M. Antonelli *et al.*, Nucl. Phys. B, Proc. Suppl. 181–182 (2008) 83 [arXiv:0801.1817].

[6] NA48/2 and P-326 status report, CERN-SPSC-2006-033.

[7] E. Goudzovski, arXiv:0804.4633 (contribution to DIS 2008 conference).

[8] S.R. Kelner, R.P. Kokoulin, A.A. Petrukhin, Phys. Atom. Nucl. **60** (1997) 576.

[9] C.H. Chen, C.Q. Geng, C.C. Lih, Phys. Rev. **D77** (2008) 014004.